METHOD FOR CALCULATION OF STRENGTH OF SIDE FRAMES OF FREIGHT WAGON BOGIES

Ramis Zaripov[1], Pavels Gavrilovs[2], Zhanar Karimova[1], Nurbolat Sembaev[1], Dinara Imangazinova[1]
[1]Toraighyrov University, Kazakhstan; [2]Riga Technical University, Latvia
ramis.zaripov@mail.ru, pavels.gavrilovs@rtu.lv, T_zhanar@mail.ru ,
n.sembaev@mail.ru , imangazinovad@mail.ru

Abstract. Despite the available achievements of science and production technologies, there is an annual increase in the number of fractures of the cast side frames of freight wagon bogies in the network, often leading to train crashes and collisions. Therefore, it is considered very important to take into account all the significant factors affecting the reduction of the resource of side frames in operation at the design stage of new structures. The aim of the work is to develop and scientifically substantiate recommendations for increasing the fatigue strength of the side frames of freight wagon bogies in operation on the basis of a refined methodology for assessing the strength of side frames, taking into account the presence of internal casting defects in dangerous sections. A method has been developed for calculating the side frames for strength, taking into account technological factors: the presence of internal casting defects in dangerous sections, mechanical properties reduced by 20% in the part, minimum wall thicknesses of the casting according to the drawing; degradation of mechanical properties for 30 years or more.

Keywords: wagon, fatigue, crack, side frame, strength.

Introduction

Metal fatigue is one of the most important causes of failures of the bearing parts of the running gear of the rolling stock in operation. Unexpected breakage of some elements, for example, the axle of a wheelset, a wheel, a side frame or a beam of a freight wagon's spring trolley, in motion can lead to tragic consequences due to the derailment of the wagon. Therefore, the study and management of the causes of fatigue failure of critical chassis parts will allow us to develop reasonable technical requirements for the quality of their manufacture, select non-destructive testing tools to identify unacceptable external and internal defects, set the size of mandatory non-destructive testing areas of parts, reduce the percentage of rejected products at manufacturing plants and at the life cycle stage, assess the impact of technological factors on reducing the fatigue strength of parts at the design stage.

A significant role in ensuring safety is also played by a reliable assessment of the fatigue strength and survivability of the structure, since the inter-repair period of the object depends on it [1].

Three element bodies are the main type of bogies for railway freight wagons in the world (in Kazakhstan the main model of freight bogies is 18-100). According to the research of many scientists [1-4], this type of bogies is morally obsolete, does not meet the requirements of speed and force impact on the railway. The situation is aggravated by the fact that there are more than 20 failures per a year of the bogie side frame on the railways of Kazakhstan and Russia [5].

The fractures of the side frames occur exclusively along the radius R55 of the inner corner of the axle box opening (Fig. 1). The causes of fractures are gross violations of the technological process of manufacturing castings, which are realized in the appearance of unacceptable internal defects of foundry origin and reduced mechanical properties of steel – strength and toughness at a temperature of -60 ºC. The ratio of these two main causes is approximately equal, if there are external casting defects and non-conforming.

Fig. 1. **Fracture of the side frame in the area of the axle box opening**

Bogie structures are loaded by a number of varying dynamic loads. Effects of such a load are concentrated in critical locations of the analysed bogie frame (e.g., points of action forces, geometry changes, welded joints etc.). The objective of the fatigue tests is verification, whether a bogie frame has sufficient fatigue strength, i.e. whether a cyclic operational load does not result in initiation of fatigue cracks or fractures [6-8].

Materials and methods

Methodology for assessing the fatigue life of cast parts of freight wagons is described in below. Let us determine the equivalent stresses in different zones of the side frame, corresponding to the damaging effect of the real spectrum of stresses in operation.

With acceptable accuracy, the linear hypothesis of A. Miner's damage can be used:

$$\sum_i \frac{n_i}{N_i} = 1 \tag{1}$$

or for the case of theoretical distribution:

$$\int_0^n \frac{dn_i}{N_i} = 1 \,. \tag{2}$$

Using the expression:

$$dn = t_H \cdot f_e \cdot \varphi(\sigma) \cdot d\sigma, \tag{3}$$

where $\varphi(\sigma)$ – density function of the distribution of amplitude values of stresses;
t_H – service life of the structure before destruction during continuous operation (movement) of the wagon;
f_e – effective (average) frequency of dynamic stress changes;

and fatigue curve equations:

$$\sigma_i^m \cdot N_i = \sigma_a^m \cdot N_0 \tag{4}$$

the condition of destruction is transformed into the following formula:

$$t_H \cdot f_e \cdot \int_0^\infty \frac{\sigma_i^m}{\sigma_a^m \cdot N_0} \cdot \varphi(\sigma) \cdot d\sigma = 1, \tag{5}$$

where n_i – number of cycles of repetition of stresses of this level;
N_i – number of stress cycles required for the destruction of parts;
σ_a – endurance limit of the structure (limiting amplitude) corresponding to the base number of cycles;
σ_j – operational stress amplitudes;

$$t_H = T_K \cdot \varepsilon, \tag{6}$$

where T_K – calendar service life of the structure;
ε – coefficient equal to 0.3 for freight wagons [9].

When the wagon is operated at the speed *v*, relative damage D_v accumulates in the structure, which is defined as:

$$D_v = t_v \cdot f_{ev} \cdot \int_0^\infty \frac{\sigma_i^m}{\sigma_a^m N_0} \cdot \varphi(\sigma) \cdot d\sigma, \tag{7}$$

where t_v – share of the total service life attributable to operation at a speed of *v*;
f_{ev} – effective frequency characteristic of a given speed *v*.

In the steady state of variable loading, damage accumulates in the structure:

$$D_v = \left(\frac{\sigma_{ev}}{\sigma_a}\right)^m . \tag{8}$$

Equating expressions (7) and (8) we get:

$$t_v \cdot f_{ev} \cdot \int_0^\infty \frac{\sigma_i^m}{\sigma_a^m \cdot N_0} \cdot \varphi(\sigma) \cdot d\sigma = \sigma_{ev}^m. \tag{9}$$

The amplitude of the stresses of the steady-state equivalent mode, taking into account the entire spectrum of operational speeds, is equal to:

$$\sigma_{ae} = \sqrt[m]{\sigma_{ev}^{m} \cdot P_v}, \tag{10}$$

where P_v − fraction of time spent on operation at the speed of v.

Taking into account the formula (9), the last expression can be represented as:

$$\sigma_{ae} = \sqrt[m]{\sum_k t \cdot \mathfrak{f}_{ev} \cdot P_v \cdot \int_0^{\infty} \frac{\sigma_i^{m} \cdot \varphi(\sigma) \cdot d\sigma}{N_0}}. \tag{11}$$

In relation to discrete distribution with a single stress amplitude, the formula (11) is written as:

$$\sigma_{aэ} = \sqrt[m]{\frac{1}{N_0} t \cdot \mathfrak{f} \cdot \sigma_i^{m}}. \tag{12}$$

Consider the probability density of the distribution of the endurance limit of the side frame ƒ(s) and the value of the equivalent stress $\sigma_{aэ}$ (Fig. 2).

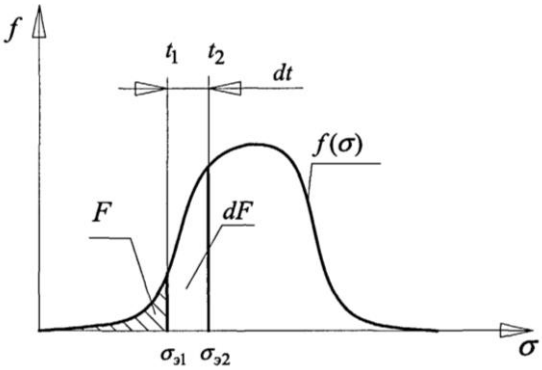

Fig. 2. **Determining the probability of failure**

The magnitude of the stress amplitude is postponed along the abscissa axis, and the probability density of the event is postponed along the ordinate axis. The graph ƒ(σ) represents the probability density distribution of failure of full-scale parts during operation [2; 9-11]. The values $\sigma_{э1}$ and $\sigma_{э2}$ are equivalent to the operational ones in terms of the damaging effect of stress at time points $t_1$and t_2. Since the probability distribution of failure is an integral function, its value at time t can be found as the area F under the probability density curve, that is, by integrating it in the specified area. Over time, *dt* increases the equivalent stress $\sigma_{э1}$ and $\sigma_{э2}$. At the same time, there is an increase in the probability of failure by the value of *dF*.

The probability that a failure will occur can be determined by the formula:

$$P(\sigma_{Э} > \sigma) = \int_0^{\sigma_э} \mathfrak{f}(\sigma) \cdot d\sigma \tag{13}$$

The number of loading cycles *n*, as well as the operating time, will be considered as a deterministic value, gradually increasing at uniform intervals. Since we introduce equivalent stresses, the time and frequency of their application, as it were, force the operational ones. To switch from the operating time in operation to the equivalent number of operating cycles, we use the formula:

$$n = k_i \cdot T, \tag{14}$$

where T – operating time of the wagon in operation, years;
k_i – transition coefficient, which physically represents the number of equivalent loading cycles in one year of actual operation.

The obtained dependences allow us to estimate the fatigue life of the side frame at given failure probabilities, that is, when the inverse problem is solved (13).

Results and Discussion

In the calculations, the finite element method has proven itself well, which makes it possible to achieve a good coincidence of the calculated and experimental data, which also has great visibility. Therefore, to determine the stress state of the side frame in the APM FEM program, its finite element model was created. The geometry of the part was approximated by volumetric 10-node finite elements with three translational degrees of freedom at each node [12]. The final elements used for the approximation were chosen with a tetrahedron-shaped geometry, since in this case it is easier to obtain a grid on a model with complex geometry. At the same time, it was assumed: the modulus of elasticity $E = 2 \cdot 10^{-5}$ MPa; Poisson's ratio $\mu = 0.3$. Fixing was carried out on the support platforms of the axle box and spring openings. The fixings are made movable to simulate the work of a real structure – the side frame is supported by movable wheel pairs.

The loads acting on the side frame during its operation can be divided into: longitudinal, transverse and vertical. Let us take a closer look at the loads at the place of application (Figure 3):

1. Vertical – support on the axle openings, loading on the lower belt of the spring opening perpendicular to the plane of the path $P_{pinning1,5,}$, $P_{vertical3}$;
2. Transverse – loading along the lower belt of the spring opening perpendicular to the direction of movement of the wagon, fixing in the box openings ($P_{transverse5,6}$, $P_{pinning4}$);
3. The force from the rasp with friction wedges along the movement of the wagon $P_{longitudinal4}$, $P_{pinning2}$;
4. Longitudinal "outward", fastening to the vertical inner surface of the spring opening in the area of the friction wedges, loading on the outer vertical support of the axle box opening along the movement of the wagon (P_{pin3},$P_{longitudinal1}$);
5. Longitudinal "inside", fastening to the vertical inner surface of the spring opening in the area of friction wedges, loading on the inner vertical support of the axle box opening along the movement of the wagon $P_{pinning2}$, $P_{longitudinal2}$.

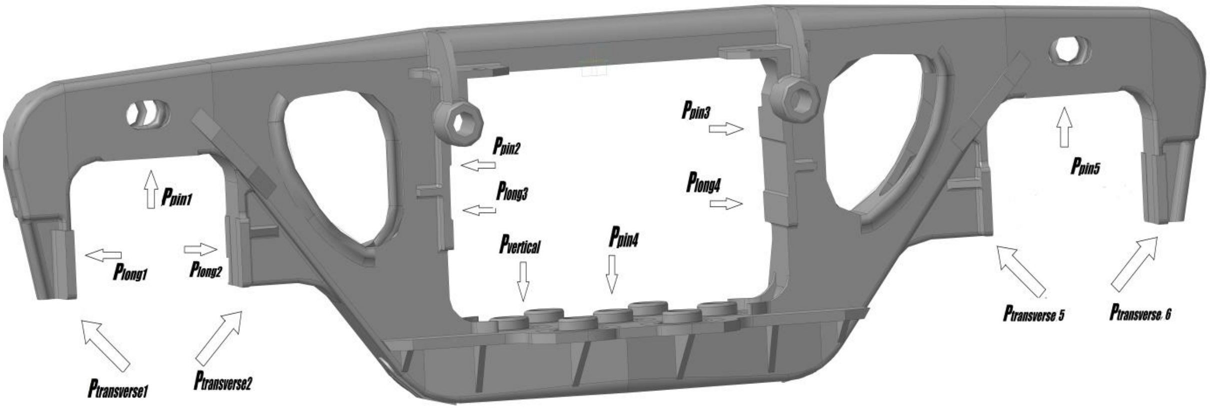

Fig. 3. **Design loads acting on the side frame**

The vertical load occurs with the following types of loading: gross gravity; vertical component from inertia forces during braking; vertical dynamic load; vertical additive from the longitudinal inertia force of the body when settling; vertical component of the force arising from the tilt of the body when the spring set subsidence.

The transverse load occurs under the following types of loading: lateral force from the guiding forces of the rails in the curve; transverse component of the longitudinal quasi-static force; frame force; lateral force resulting from the elevation of the outer rail in the curve. The longitudinal load occurs under the following types of loading: inertia force of the mass of the wheelset; longitudinal load during braking; longitudinal force arising from the friction between the wheels and rails in the curve.

Fig. 4-6 shows the fields of equivalent stress distributions according to the Mises for three cases of loading of the side frame No. 100.00.002-4 (on the left in Fig. 4-7, the side frame with a box section of the outer column of the box opening of the new design) and No. 100.00.002-2 (on the right in Fig. 4-6, the side frame with an I-beam section of the outer column of the box opening of the old design). To assess the operating stresses, the calculation of the side frame was carried out for three types of normative loads: longitudinal load during braking (P_{break} = 42.5 kN), gross gravity, ($P_{g\ r}$ = 212.6 kN), frame force, P_{f} = 55.3 kN) [13].

The results of the finite element analysis reflected in these figures show the redistribution of stresses across the zones of the outer axle box angle, the over-axle opening and the inner corner of the axle box opening on the side frames of different structures under the same operating loads. In the case of vertical loading in the frame of the new design (Fig. 4-6, a) in comparison with the old one (Fig. 4-6, b), the stresses in the superstructure increased, the remaining stress values remained unchanged. With transverse and longitudinal loading, the stresses in the outer lateral angle of the side frame decreased (Fig. 4-6, a) in comparison with the old side frame by 10-15% (Fig. 4-6, b). The designs of the two frames differ only in the execution of the outer angle of the jaws, the rest of the part remained without significant changes, therefore, only the three specified zones in the frame axle opening were taken as a comparison.

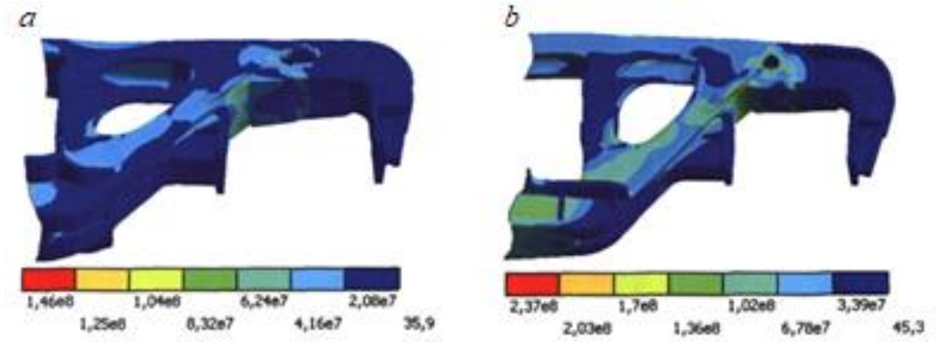

Fig. 4. **Distribution of stress fields for the new (a) and old (b) frame structure (MPa) for the case of vertical loading**

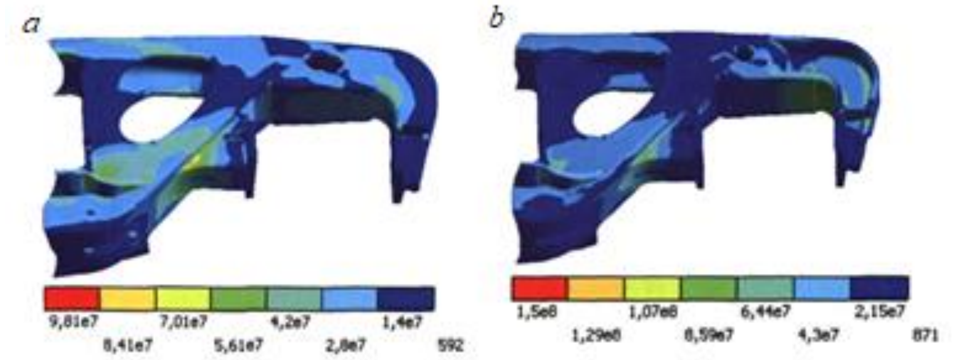

Fig. 5. **Distribution of stress fields for the new (a) and old (b) frame structure (MPa) for the case of transverse loading**

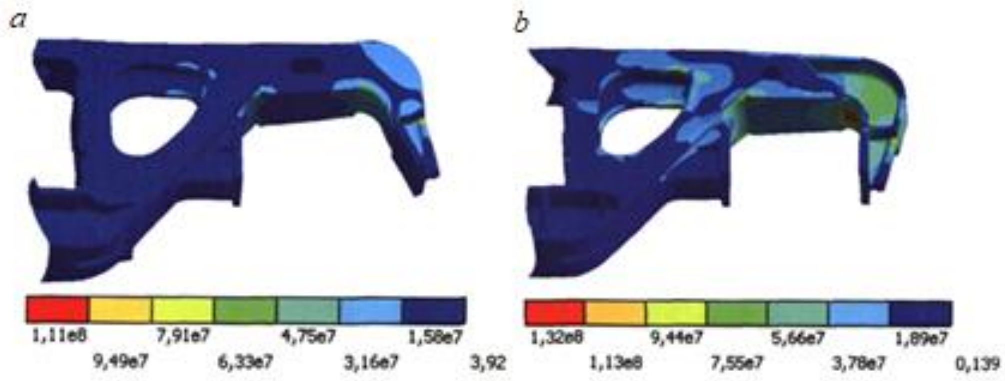

Fig. 6. **Distribution of stress fields for the new (a) and old (b) frame structure (MPa) of longitudinal loading**

Table 1 shows the calculation results separately for the frame with an I-beam section and separately with a box section of the outer column of the axle opening.

Table 1

Operating stress in the side frame zones (MPa)

Name of the design load	Old construction			New construction		
	Zones on the side frame					
	1	2	3	4	5	6
Longitudinal load during braking	100	15	65	55	10	35
Gross gravity	-	70	110	-	107	110
Frame force	90	35	20	33	10	14

From the analysis of Table 1 and the data of operational failures (Table 2), we also see that the redistribution of cracks arising correlates well with the redistribution of the stress state of the compared frames.

Table 2

Distribution of the side frame failures by zones

Year of the survey	Distribution of cracks by zones on the side frame, % of the total		
	1	2	3
2004	35.2	17.5	39.6
2014	27.3	25.0	12.7
2020	23.5	28.2	10.9

One of the factors affecting the stressed state of the part is the resonance of the natural oscillation frequency with the frequency of external load application. For the purpose of verification, a modal analysis was carried out to find the natural oscillation frequencies of the side frame. The calculation showed that the minimum oscillation frequency is 94.5 Hz, the first oscillation form is shown in Fig. 7. The first form of the natural oscillation frequency of the side frame coincides with the transverse loading of the part [14]. But the natural oscillation frequency of the part significantly exceeds the effective loading frequency, therefore, the effect of frequency overlap in the calculation of the stressed state of the part cannot be taken into account.

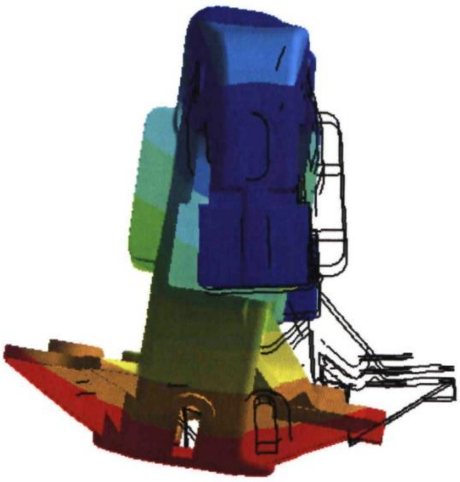

Fig. 7. **First form of vibration of the side frame**

Since the change in operating stresses and the number of failures correlate with each other, having found the dependence of stresses in different zones of the side frame on various forces and knowing the nature of damage to the part in operation, we will determine the nature of the operating loads. But depending on the number of cycles and the magnitude of the applied loads there is both a lot and low-cycle fatigue damage to the part material, which significantly complicates the calculations. In addition, the loads have a random distribution spectrum. Therefore, to assess the loading of the side frame, we introduce the value of the stress σ_{eq}, which is "averaged" and corresponds to the destructive effect of the real stress spectrum, but has a simple sinusoidal or sawtooth appearance. Assume that all loads act constantly, with a constant amplitude value, the same frequency, and all at the same time.

Take the value $\sigma_{j\ eq}$ stress amplitude for the j-th zone of the side frame. For zones where the average load has a value different from that applied during testing, it is necessary to introduce an additional value to the stress amplitude that would take this into account. According to [3], the additional value can be determined by the formula:

$$\Delta = \Psi \cdot (P_{awer} + P_{set} \cdot K_u) \tag{15}$$

where Ψ – sensitivity coefficient of the part to the asymmetry of the cycle, it is assumed for side frames made of normalized steel 20GL equal to 0.05;
K_u – load capacity utilization factor, equal to 0.9;
P_{awer} – value of the average load (stress);
P_{set} – calculated value of the load (stress), with which P_{awer} is compared.

The magnitude of the stresses $\boldsymbol{\sigma_{ji}}$ in the *i*-th zone of the side frame from the action of the force $\boldsymbol{P_i}$ is determined from the ratio

$$\sigma_{ji} = k_{ji} \cdot P_i, \tag{16}$$

where P_i – magnitude of the load applied at the i-th point of the side frame;
k_{ji} – coefficient of proportionality between the stress σ_{ji} in the *j*-th zone of the side frame from the action of the force P_i applied at the *i*-th point of the side frame.

According to the hypothesis of the independence of the action of forces on the part, the stress in the *j*-th zone of the side frame from the action of forces applied at several points of the side frame [15]:

$$\sigma_\Sigma = \sum_i \sigma_{ji} = \sum_i k_{ji} \cdot P_i \tag{17}$$

The operational probability of failure in the expanded form has the following form:

$$F(t) = \frac{1}{\sqrt{2\pi}} \int_0^{\frac{lgt-a}{b}} \cdot e^{-\frac{x^2}{2}} dx + 0{,}5 \tag{18}$$

At the same time, the probability of failure in the *j*-th zone under the action of unknown amplitude forces $\boldsymbol{P_i}$ according to (12), (13) and (17) can be represented as:

$$F\,(t) = \frac{1}{\sqrt{2\pi}} \int_0^{\frac{\Sigma k_{ji} P_i \sqrt[m]{t-c}}{d}} \cdot e^{-\frac{x^2}{2}} dx + 0{,}5 \tag{19}$$

Since the forcing coefficient is set during tests, in the formula (19) the values $\boldsymbol{N_0}$ and *f* dependent on it are conditionally assumed to be equal to one, and in the final calculations the forces are specified according to the formula (12). Comparing the probabilities (18) and (19) we see that they differ only in the limits of integration. Considering this, as well as the fact that with the simultaneous action of the amplitude forces $\boldsymbol{P_i}$, the equality of expressions (18) and (19) must be fulfilled for each of the *j*-th zones of the side frame, we obtain a system of equations

$$P_i = \left\{ \begin{array}{c} \frac{\lg(t)-a_1}{b_1} = \frac{(k_{11}P_1 + k_{12}P_2 + \dots k_{1i}P_i)\cdot \sqrt[m]{t-c}}{d} \\ \frac{\lg(t)-a_2}{b_2} = \frac{(k_{21}P_1 + k_{22}P_2 + \dots k_{2i}P_i)\cdot \sqrt[m]{t-c}}{d} \\ \dots\dots \\ \frac{\lg(t)-a_j}{b_j} = \frac{(k_{ji}P_1 + k_{ji}P_2 + \dots k_{ji}P_i)\cdot \sqrt[m]{t-c}}{d} \end{array} \right\} \tag{20}$$

Having calculated the loads $\boldsymbol{P_i}$ according to the formula (20), we obtain an estimate of the dynamic loading of the cast parts of the trolley in operation. Substituting the obtained forces into the formula (13), we obtain a methodology for assessing the fatigue endurance of an analog part (for example, parts with increased fatigue strength).

Conclusions

According to the results of the research the following can be noted**.**

1. The parameters of the probability distribution of the failure-free operation of the side frame at a given load value were obtained based on the results of fatigue bench tests.
2. A methodology has been developed for assessing the fatigue life of cast parts in operation, taking into account the dispersion of the strength characteristics of the part and allowing to find stresses equivalent to operational ones.
3. A technique has been developed that makes it possible to estimate the amplitude dynamic loads equivalent in damaging effect to the real spectrum of forces acting on the side frame over its entire service life.
4. The obtained dependencies make it possible to estimate the resource of a new part at the design and manufacturing stages.

References

[1] Lagerev I. A. Evaluation of fatigue strength and survivability of the side frame cast truck freight car/ Bryansk State University (Bryansk, Russian Federation) DOI: 10.22281/2413-9920-2017-03-04-374-380 (In Russion)
[2] Ognevoy V. Ya. Fractometrical particular fracture cast side frames freight car bogies/Polzunovskiy almanah, 2011. No 4. 36-41. (In Russian).
[3] Pranov V. A. Methodology for assessing the operational reliability of cast parts of a freight car trolley // Transport of the Urals. - 2011. – No 2 (29). - pp. 56-61(In Russian).
[4] Freimane J., Mezitis M., Mihailovs F. Maneuver Movements' Safety Increase Using Maneuver Locomotive Identification and Distance Control (2016) Procedia Computer Science, 104, pp. 375-379.
[5] Domin R., Gorbunov N., Nogenko O., Kara S., Gryndei P., Mokrousov S., Chernikov V. Concepts of modern bogies for railway freight wagon Commission of motorization and energetics in agriculture – 2015, Vol. 15, No.2, 45-50 (in Russion)
[6] Dizo J., Blatnicky M., Harusinec J., Pavlik A., Smetanka L. Strength analysis of a freight bogie frame under the defined load cases Communications - Scientific Letters of the University of Zilina 2018, 20(4), pp. 58-62. DOI: 10.26552/com.C.2018.4.58-62
[7] Willenborg J.J. A Crack Growtli Retardation Model Using an Effective Stress Concept/J.J. Willenborg, K.M. Fngle, N.A. Wood // AFFDL-TR-71-1. – 1971.
[8] Harak S.S., Sharma S.C., Harsha S.P. Structural Dynamic Analysis of Freight Railway Wagon Using Finite Element Method. Procedia Material Science. 2014, 6, pp. 1891-1898.
[9] Šťastniak P., Moravčík M., Smetanka L., Baran P. Strength Investigation of Main Frame in New "Track friendly" Railway Bogie/ Manufacturing technology, April 2018, Vol. 18, No. 2
[10] Yatsun V., Filimonikhin G., Haleeva A., Krivoblotsky L., Machok Y., Mezitis M., Podoprygora N., Sadovyi M., Strautmanis G. Searching for the twofrequency motion modes of a three-mass vibratory machine with a vibration exciter in the form of a passive auto-balancer (2020) Eastern-European Journal of Enterprise Technologies, 4 (7-106), pp. 103-111.
[11] Strautmanis G., Mezitis M., Strautmane V. The impact of rotor elastic suspension settings on the acceleration of the automatic balancer compensating mass (2017) Vibroengineering Procedia 14 pp. 13-17.
[12] Pr EN 12663.2:2007. Railway applications – structural requirements of railway vehicle bodies.
[13] Stichel S. "On freight wagon dynamics and track deterioration," Journal of rail and Rapid Transit, vol. 213, 1999.
[14] Eurocode 3: Design of steel structures. – Pt. 1.9 BSEN 1993-1-9: Fatigue. (It was approved European Committee for Standardization on 16 Apr. 2004).
[15] Rizvi D. R. Optimisation of Bogie Springs for Higher Axle Load Wagons/D. R. Rizvi P. K. Bharti // Intern. J. of Engineering Research & Technology. – 2015. – Vol. 4. – Iss. 05. – pp. 56-60. DOI: 10.17577/ijertv4is050162.